

LETTER TO THE EDITOR

Viscoelastic properties of attractive and repulsive colloidal glasses

Antonio M Puertas¹, Emanuela Zaccarelli² and Francesco Sciortino²

¹ Group of Complex Fluids Physics, Department of Applied Physics, University of Almeria, 04120 Almeria, Spain

² Dipartimento di Fisica and INFM Udr and SOFT: Complex Dynamics in Structured Systems, Universita' di Roma La Sapienza, Piazzale Aldo Moro 5, I-00185 Rome, Italy

E-mail: apuestas@ual.es

Received 15 March 2005, in final form 15 May 2005

Published 10 June 2005

Online at stacks.iop.org/JPhysCM/17/L271

Abstract

We report a numerical study of the shear viscosity and the frequency dependent elastic moduli close to dynamical arrest for a model of short range attractive colloids, both for the repulsive and the attractive glass transition. Calculating the stress autocorrelation functions, we find that density fluctuations of wavevectors close to the first peak in the structure factor control the viscosity rise on approaching the repulsive glass, while fluctuations of larger wavevectors control the viscosity close to the attractive glass. On approaching the glass transition, the viscosity diverges with a power law with the same exponent as the density autocorrelation time.

(Some figures in this article are in colour only in the electronic version)

Colloidal dispersions, in addition to their technological relevance, play an important role in the development of basic physical sciences, in particular in the fascinating field of formation of disordered arrested states, glasses and gels. The possibility of tailoring shape, size and structure of the colloidal particles makes it possible to design specific interparticle interaction potentials. Recently, the application of experimental [1–3] and theoretical tools [4–6] to the analysis of the glass transition in short-ranged attractive colloids has shown an extremely rich scenario, with no analogue in atomic systems [7]. The standard packing-driven hard-sphere glass transition transforms—discontinuously in some cases—into a novel type of glass transition driven by the short-range attractions. The connection between this attractive transition and gelation is still a matter of debate.

Previous numerical work on short-range attractive colloids has mostly focused on the behaviour of single-particle diffusion and on the time dependence of the density autocorrelation function $\Phi_q(t)$ close to dynamical arrest. Despite the strong link with experiments and the relevance to industrial applications, the numerical evaluation of the viscosity η and viscoelastic properties $\tilde{\eta}(\omega)$ has not been performed, since significant computational effort is required for

accurate calculation of $\tilde{\eta}(\omega)$, even more for states close to dynamical arrest. The behaviour of η close to dynamical arrest in colloidal systems is under theoretical and experimental investigation [8–11]. Measurements in dense hard sphere colloids show a divergence of η in the vicinity of the repulsive glass point, its exact location and functional form being still under debate [10, 12]. For colloidal gels, a power law divergence has been reported at the gel transition [13]. The mode coupling theory (MCT) for glass transitions [14], which anticipated the presence of novel dynamic phenomena in short-range attractive colloids [4–6], predicts asymptotic power law divergence of η with the distance to the transition, with identical exponents to the divergence of the timescale, and the inverse of the diffusion coefficient.

In this letter we report an extensive numerical study of the viscoelastic behaviour of a colloidal system, approaching both the repulsive and the attractive glass transition. We concentrate on the effects arising from direct interactions among colloids, and neglect the contributions from the solvent (both solvent viscosity and hydrodynamic interactions), which are not expected to present divergences close to the transition points. We calculate the stress autocorrelation function, as well as the viscosity and the elastic moduli. Close to both transitions, η diverges with a power law, with the same exponent as the density relaxation time, but different from that of the diffusion coefficient. Moreover, we provide evidence that the rise of η is controlled by density fluctuations of wavevectors around the first peak in the structure factor close to the repulsive glass, and larger wavevectors for the attractive glass.

Our system is polydisperse, composed of 1000 particles interacting via a steep repulsive (r^{-36}) potential complemented by the Asakura–Oosawa (AO) short-range attractive potential³. The attraction strength is measured in units of the polymer volume fraction, ϕ_p , and density is reported as colloid volume fraction, $\phi_c \equiv 4/3\pi a[a^2 + \delta^2]\rho$, with ρ the number density, a the mean radius and δ the width of the size distribution, $\delta = 0.1a$, and the range of the interaction is $\xi = 0.1a$. A long-range repulsive barrier is added to inhibit liquid–gas separation at high attraction strength. The specific shape of the potential can be found in [16]. Lengths have been measured in units of a , the particle mass is set to $m = 1$, and $k_B T = 4/3$.

Dynamics in this model has been studied previously [16, 17]. In the absence of polymers ($\phi_p = 0$) and with no repulsive barrier, on increasing the particle packing fraction a repulsive glass transition is observed at $\phi_c^G \simeq 0.594$. At fixed $\phi_c = 0.40$, on increasing ϕ_p , an attractive glass transition is observed at $\phi_p^G \simeq 0.4265$. Both values were obtained from the MCT analysis for $\Phi_q(t)$ and D_0 (power-law fittings) [16, 17].

The shear viscosity η is given by the Green–Kubo relation

$$\eta \equiv \int_0^\infty dt C_{\sigma\sigma}(t) = \frac{1}{3Vk_B T} \int_0^\infty dt \sum_{\alpha < \beta} \langle \sigma^{\alpha\beta}(t) \sigma^{\alpha\beta}(0) \rangle, \quad (1)$$

which expresses η as the integral of the correlation function of the non-diagonal terms of the microscopic stress tensor, $\sigma^{\alpha\beta} = \sum_{i=1}^N m v_{i\alpha} v_{i\beta} - \sum_{i < j}^N \frac{r_{i\alpha} r_{j\beta}}{r_{ij}} V'(r_{ij})$, where V is the volume of the simulation box, $v_{i\alpha}$ is the α th component of the velocity of particle i , and V' is the derivative of the total potential.

We have performed Newtonian dynamics (ND) and Brownian dynamics (BD) simulations, to test the independency of the long time dynamics on the short time model⁴. Although the latter is more appropriate for colloidal systems, its short timescale is much smaller, implying larger computational effort. The inset in figure 1 shows $C_{\sigma\sigma}(t)$ for two states with $\phi_c = 0.40$, both for ND and BD. In the case of ND, clear oscillations in $C_{\sigma\sigma}(t)$ at small time ($t < 0.5$) are observed, caused by motion in the attractive well. These oscillations are completely

³ The AO potential is an effective attractive interaction between colloids, induced by small polymers in the mixture; see e.g. [15].

⁴ A high friction coefficient ($\gamma = 50$) is needed to decouple momentum relaxation from the effect of the attractions.

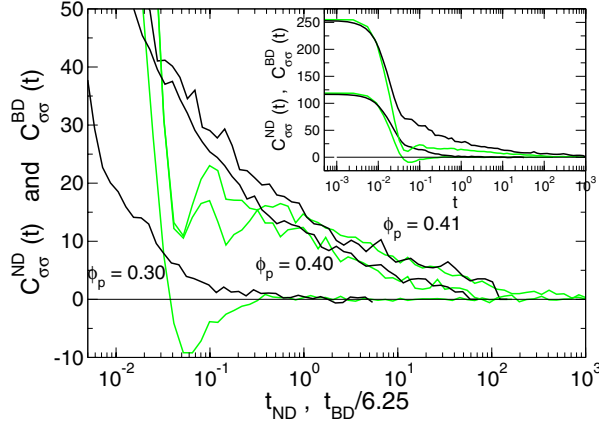


Figure 1. Stress correlation functions for ND (grey (green) lines) and BD (black lines), time rescaled, for different states. In all cases, $C_{\sigma\sigma}^{BD}(t)$ has been time-rescaled onto $C_{\sigma\sigma}^{ND}(t)$ by a factor 6.25. Inset: full scale stress correlation functions for ND and BD (without time rescaling); $\phi_p = 0.30$ and 0.41 .

damped in the BD case, confirming that this part of the decay of the correlation function has a microscopic (dynamic-dependent) origin and that short time oscillations are not to be expected in real colloidal systems. When ϕ_p is increased, an additional slow relaxation process is present. Interestingly, the BD $C_{\sigma\sigma}(t)$ can be time-rescaled to collapse on ND data (main figure) at long times by a constant factor for all states, confirming that the long time dynamics of the system does not depend on the microscopic dynamics, in agreement with previous studies in glass forming atomic systems [18]. Therefore, we use the more efficient ND hereafter to analyse the long time decay of $C_{\sigma\sigma}(t)$ and the viscosity close to both transitions.

Figure 2 shows the stress correlation function, $C_{\sigma\sigma}(t)$, for different ϕ_c or ϕ_p values on approaching the repulsive (upper panel) and attractive (lower panel) glass transitions. Correlation functions have been superimposed by a suitable scaling of time. On approaching the transition, $C_{\sigma\sigma}(t)$ slows down by several orders of magnitude—with no appreciable change in its shape at long time—causing the rise of η . A stretched exponential can be fitted to the decay with an exponent $\beta = 0.48$ and 0.25 for the repulsive and attractive glasses, respectively.

The scaling property of $C_{\sigma\sigma}(t)$ at long times is reminiscent of the scaling of $\Phi_q(t)$. Indeed, within MCT, $C_{\sigma\sigma}(t)$ can be related to $\Phi_q(t)$, by means of [19, 20]:

$$C_{\sigma\sigma}(t) = \frac{k_B T}{60\pi^2} \int_0^\infty dq q^4 \left[\frac{d \ln S_q}{dq} \Phi_q(t) \right]^2 \quad (2)$$

where S_q is the static structure factor. Accordingly, the timescales from $C_{\sigma\sigma}(t)$ and $\Phi_q(t)$ should be equivalent. The two insets of figure 2 show a plot of τ_σ versus τ_q , parametric in ϕ_c or ϕ_p ; here τ_σ is defined as $C_{\sigma\sigma}(\tau_\sigma) = 1$ for the repulsive glass and $C_{\sigma\sigma}(\tau_\sigma) = 5$ for the attractive one, and $\Phi_q(\tau_q) = f_q/e$ with f_q the non-ergodicity parameter gives τ_q . In both transitions, τ_q and τ_σ are proportional to each other (continuous lines), showing that they are indeed equivalent.

The dominant contribution to the q -integral in equation (2), for times in the α -decay of $\Phi_q(t)$, can be revealed studying the function $q^4 [d \ln S_q / dq f_q]^2$. This function oscillates with q (from $d \ln S_q / dq$), but its envelope shows a maximum. For the repulsive glass transition, this maximum is close to the nearest neighbour peak of S_q ($qa \approx 3.75$), and it is located at higher q for the attractive one. (For the AO potential, using Percus–Yevick closure, the dominant wavevector is $qa \approx 13$, although the distribution is very wide.)

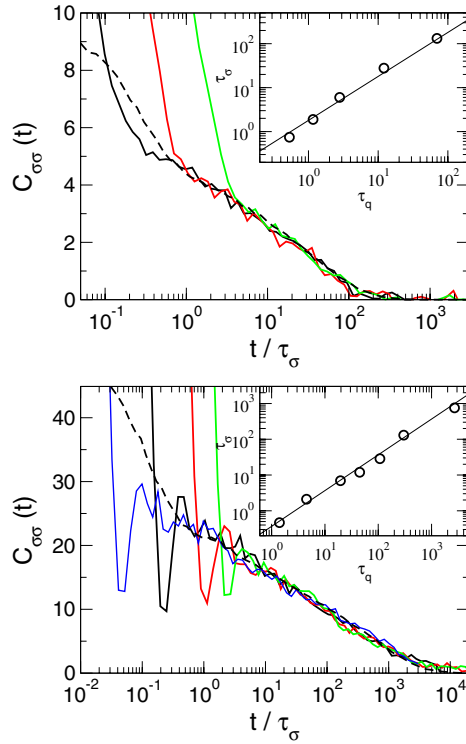


Figure 2. Stress correlation functions for different states approaching the glass transitions. Upper panel: repulsive glass transition. From right to left: $\phi_c = 0.55, 0.57, 0.58$. Lower panel: attractive glass transition. From right to left: $\phi_p = 0.405, 0.41, 0.415, 0.42$ and $\phi_c = 0.40$. The dashed lines are $\Phi_q(t)^2$ for $qa = 4$ at $\phi_c = 0.58$ (repulsive glass) and $qa = 11$ at $\phi_p = 0.415$ (attractive glass). Insets: timescale from the stress correlator τ_σ versus timescale from the density correlator τ_q at the wavevectors given above.

To test this, we have compared $C_{\sigma\sigma}(t)$ with Φ_q^2 (evaluated from the simulations) at different wavevectors, allowing for a scaling factor only in the amplitude. Good agreement is obtained for $qa = 4$ in the repulsive glass transition and $qa = 11$ in the attractive one (dashed lines in figure 2). This comparison shows that, indeed, the long time decay of the stress correlation function, within the accuracy of our numerical results, is adequately described by the dominant wavevector in equation (2).⁵ Interestingly, the wavevectors driving the repulsive and the attractive ideal glass transitions, as observed from $\Phi_q(t)$, are also the dominant ones in the calculation of $C_{\sigma\sigma}(t)$, respectively.

We now turn to the study of η , which is more efficiently calculated numerically using the Einstein relation [21]:

$$\eta = \frac{1}{6Vk_B T} \lim_{t \rightarrow \infty} \frac{1}{t} \langle \Delta A(t)^2 \rangle, \quad (3)$$

where $\Delta A(t)$ is the integral from zero to t of the three off-diagonal terms of the stress tensor. Figure 3 shows the behaviour of η approaching the repulsive and the attractive glass transitions,

⁵ The identification of the decay of $C_{\sigma\sigma}$ with a single Φ_q is of course an approximation. Indeed, different q are characterized by stretched exponential decay with different values of τ_q and β_q . Slow decaying contributions (q around the nearest neighbour peak of $S(q)$) will always control the decay of $C_{\sigma\sigma}$ at very long times for both glass transitions. In the present simulations, however, such an effect is not observed within the accuracy of our data.

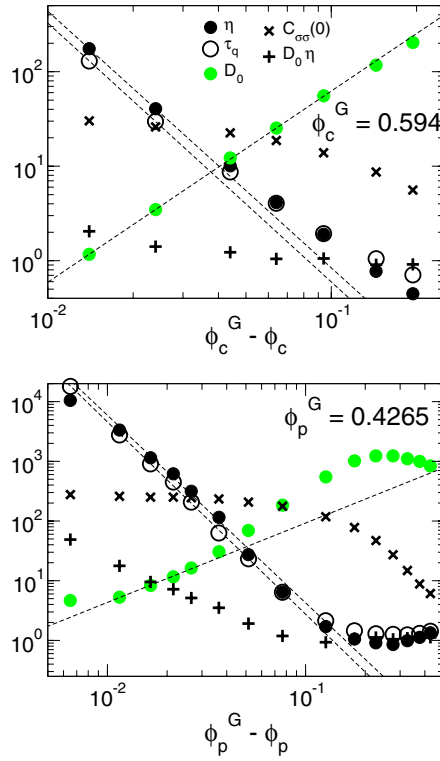


Figure 3. Viscosity, η , timescale at $qa = 3.5$, τ_q , and diffusion coefficient ($D_0 \times 10^3$) and $C_{\sigma\sigma}(0)$ for the repulsive glass transition (upper panel) and the attractive one (lower panel), as labelled. Note that ηD_0 diverges in the transition point. The lines are the power law fittings to η , τ_q and D_0 (see table 1).

Table 1. Exponents obtained in fitting η , τ and $1/D_0$ to $(\phi_c^G - \phi_c)^{-\gamma}$, for the repulsive glass and $(\phi_p^G - \phi_p)^{-\gamma}$ for the attractive one.

	γ_η	γ_τ	γ_{D_0}	γ_{MCT}
Repulsive glass	2.72	2.74	2.02	2.58 [23]
Attractive glass	3.14 ^a	3.23	1.33	2.95 ^b

^a The last point, $\phi_p = 0.42$, is not considered in the fitting, due to the large numerical error in determining η .

^b This value was calculated for a square well with a width of 0.03 diameters.

as a function of the distance to the transition points, ϕ_c^G and ϕ_p^G [16, 17]. For both the repulsive and attractive glass transitions, η is well described by a power law, diverging at the same points as τ_q . In the attractive case, η shows a minimum for intermediate ϕ_p , arising from the competition of the two arrest mechanisms [1, 22].

Figure 3 also shows τ_q for $qa = 3.5$ (the nearest neighbour peak in S_q), the long time self-diffusion coefficient, D_0 , $C_{\sigma\sigma}(0)$ and ηD_0 . For both transitions, both τ_q and D_0 are linear in the log–log plot and hence can also be well described by power laws. While $\eta \sim \tau_q$, as confirmed by the constant ratio η/τ_q (not shown), the product ηD_0 shows a clear trend, indicating that the power-law exponents are very similar for η and τ_q but different for D_0 . The best-fit exponents are reported in table 1 for both transitions, together with the MCT predictions

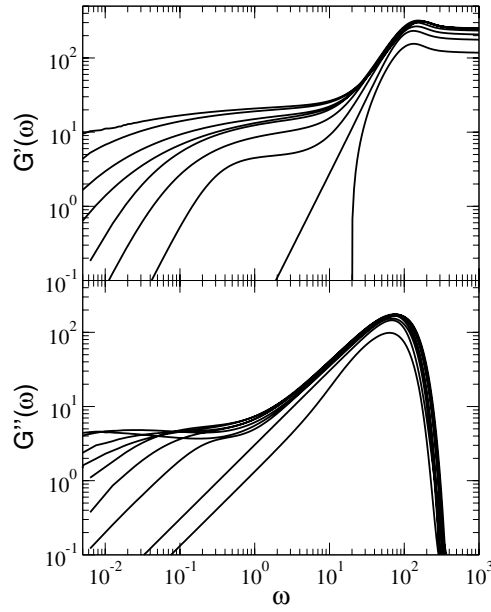


Figure 4. Elastic (upper panel) and viscous (lower panel) modulus for different states approaching the attractive glass transition at $\phi_c = 0.40$: from right to left $\phi_p = 0.30, 0.35, 0.375, 0.39, 0.40, 0.405, 0.41, 0.415, 0.42$.

for the HS case and for a short-ranged square well potential (with attractive width 3% the value of the total interaction range). From a MCT point of view, short-range attractive potentials are characterized by γ exponents larger than the HS case, whose actual value depends on the details of the potential. Data in table 1 confirm that for the attractive glass, the exponents are larger than the HS case, while for the repulsive glass, the exponents agree with the HS MCT predictions.

The difference between the exponents γ_η and γ_{D_0} indicates that the Stokes–Einstein relationship breaks down not only in the form $D_0\tau$, as already shown in many different systems, but also in the form $D_0\eta$. This breakdown, much more evident in the attractive glass case, is not consistent with MCT, although the theory correctly predicts the similarity between the exponents of τ_q and η . The power-law divergence of η at the attractive glass transition agrees with recent experimental observations in colloidal gels [13]. It is also consistent with recent interpretation of data for the repulsive glass transition [12], although this analysis is not conclusive, since an exponential divergence around $\phi_m = 0.64$ has also been proposed [10]. The constant $C_{\sigma\sigma}(0)$ is the elastic modulus at infinite frequency G'_∞ . As both transitions are approached, it tends to a finite value without showing any divergence, also in agreement with MCT.

To make direct contact with experiments, we calculate $\tilde{G}(\omega) \equiv i\omega\tilde{\eta}(\omega) = G'(\omega) + iG''(\omega)$, where $\tilde{\eta}(\omega)$ is the Fourier transform of $C_{\sigma\sigma}(t)$. To minimize numeric noise, we fit $C_{\sigma\sigma}(t)$ using functional forms that capture the fast short time behaviour and a long time stretched exponential decay⁶. Figure 4 shows the resulting $\tilde{G}(\omega)$ for the attractive glass transition case. Similar qualitative features are observed for the repulsive case. An incipient plateau

⁶ Short time behaviour: $G_\infty/(1+At^2)$ for the repulsive glass and $G_\infty \exp\{-At^2\}$ for the attractive one. The observed long time scaling property (figure 2) imposes equal values of the stretching exponent for all ϕ_p .

at low frequencies in $G'(\omega)$ and a secondary maximum in $G''(\omega)$ appear on approaching ϕ_p^G , leaving a minimum at intermediate frequencies. Both features are consistent with MCT predictions [24, 25] and observed in experiments of hard sphere colloids [26] and attractive systems [11, 13]. The short time behaviour of $C_{\sigma\sigma}(t)$ causes the sharp increase in $G'(\omega)$ at $\omega \sim 10^1$ for $\phi_p = 0.30$, which thus should not be expected in colloidal systems.

To conclude, we have shown that the viscosity diverges as the repulsive or the attractive glass transitions are approached, following a power law with the same exponent as the timescale from the density autocorrelation function. It should be acknowledged, however, that this behaviour is found ‘far from the transitions’, and we expect corrections entering closer to the transition, as observed for other correlation functions in many different glass forming systems. This letter, thus, provides further evidence of the applicability of MCT to slow dynamics in colloidal systems in this regime, in agreement with some experiments.

We thank P Tartaglia for useful discussions and M Fuchs, M Cates and W Götze for careful reading of the manuscript. AMP thanks the Dipartimento di Fisica at the Università di Roma ‘La Sapienza’, where this work was carried out, for hospitality and the Spanish Ministerio de Educacion, Cultura y Deporte for financial support. EZ and FS acknowledge support from Miur FIRB, Cofin and MRTN-CT-2003-504712.

References

- [1] Pham K *et al* 2002 *Science* **296** 104
Pham K *et al* 2004 *Phys. Rev. E* **69** 011503
- [2] Eckert T and Bartsch E 2002 *Phys. Rev. Lett.* **89** 125701
- [3] Chen S-H, Chen W-R and Mallamace F 2003 *Science* **300** 619
- [4] Dawson K *et al* 2001 *Phys. Rev. E* **63** 011401
- [5] Bergenholtz J and Fuchs M 1999 *Phys. Rev. E* **59** 5706
- [6] Fabbian L *et al* 1999 *Phys. Rev. E* **59** R1347
Fabbian L *et al* 1999 *Phys. Rev. E* **60** 2430
- [7] Sciortino F 2002 *Nat. Mater.* **1** 145
- [8] Fuchs M and Cates M E 2002 *Phys. Rev. Lett.* **89** 248304
- [9] Miyazaki K and Reichman D R 2002 *Phys. Rev. E* **66** 050501
- [10] Cheng Z *et al* 2002 *Phys. Rev. E* **65** 041405
- [11] Mallamace F *et al* 2004 *J. Phys.: Condens. Matter* **16** S4975
- [12] General discussion 2003 *Faraday Discuss.* **123** 303
- [13] Shah S A, Chen Y-L, Schweizer K S and Zukoski C F 2003 *J. Chem. Phys.* **119** 8747
- [14] Götze W 1991 *Liquids, Freezing and Glass Transition* ed J P Hansen, D Levesque and J Zinn-Justin (Amsterdam: North-Holland) p 287
- [15] Likos C N 2001 *Phys. Rep.* **348** 267
- [16] Puertas A M, Fuchs M and Cates M E 2003 *Phys. Rev. E* **67** 031406
- [17] Voigtmann Th, Puertas A M and Fuchs M 2004 *Phys. Rev. E* **70** 061506
- [18] Gleim T, Kob W and Binder K 1998 *Phys. Rev. Lett.* **81** 4404
- [19] Bengtzelius U, Götze W and Sjölander A 1984 *J. Phys. C: Solid State Phys.* **17** 5915
- [20] Nägele G and Bergenholtz J 1998 *J. Chem. Phys.* **108** 9893
- [21] Allen M P and Tildesley D J 1987 *Computer Simulation of Liquids* (Bristol: Clarendon)
- [22] Foffi G *et al* 2002 *Phys. Rev. E* **65** 050802
- [23] Barrat J L, Gotze W and Latz A 1989 *J. Phys.: Condens. Matter* **1** 7163
- [24] Fuchs M and Mayr M R 1999 *Phys. Rev. E* **60** 5742
- [25] Dawson K A *et al* 2001 *J. Phys.: Condens. Matter* **13** 9113
- [26] Mason T G and Weitz D A 1995 *Phys. Rev. Lett.* **75** 2770